Deep-Sea Research II 93 (2013) 84–95

Contents lists available at SciVerse ScienceDirect

Deep-Sea Research II

journal homepage: www.elsevier.com/locate/dsr2

Variability of chromophytic phytoplankton in the North Pacific Subtropical Gyre

Binglin Li [a], David M. Karl [a], Ricardo M. Letelier [b], Robert R. Bidigare [c], Matthew J. Church [a,*]

[a] Department of Oceanography, University of Hawaii, 1000 Pope Road, Honolulu, HI 96822, United States
[b] College of Oceanic and Atmospheric Sciences, Oregon State University, 104 COAS Administration Building, Corvallis, OR 97331, United States
[c] Hawaii Institute of Marine Biology, University of Hawaii, PO Box 1346, Kaneohe, HI 96744, United States

ARTICLE INFO

Available online 6 March 2013

Keywords:
North Pacific
Station ALOHA
Phytoplankton
Oligotrophic
Pelagophytes
Diatoms
Prymnesiophytes

ABSTRACT

Eukaryotic phytoplankton play important roles in regulating productivity and material export in oligotrophic ocean ecosystems. In this study, we examined the vertical and temporal variability in planktonic Chromalveolate (hereafter chromophyte) assemblages over a 2-year period (2007–2009) at Station ALOHA (22°45′N, 158°W) in the North Pacific Subtropical Gyre (NPSG). Polymerase chain reaction (PCR) amplification, cloning, and sequencing of form ID *rbcL* genes from samples collected at nearly monthly intervals provided information on the diversity, abundances, and variability associated with chromophytic phytoplankton. Despite persistently oligotrophic conditions, the euphotic zone of this habitat supported a phylogenetically diverse assemblage of chromophytic algae, including representatives of various genera of diatoms, pelagophytes, prymnesiophytes, and dinoflagellates. Quantitative PCR (qPCR) amplification of diatom, prymnesiophyte, and pelagophyte *rbcL* phylotypes revealed that the population structure of these assemblages was highly variable in time, with gene abundances often varying more than an order of magnitude between successive months. Diatom *rbcL* genes were typically the most abundant in both the upper and lower regions of the euphotic zone, while *rbcL* gene abundances of the prymnesiophytes and pelagophytes were significantly greater (One-way ANOVA, $P < 0.05$) in the lower regions of the euphotic zone (75–125 m) than in the upper euphotic zone (5–45 m). Similarly, we observed elevated concentrations of 19-hexanoxyfucoxanthin and 19-butanoxyfucoxanin (diagnostic pigments of prymnesiophytes and pelagophytes, respectively) in the lower euphotic zone, while concentrations of fucoxanthin (a diagnostic diatom pigment) demonstrated less vertical structure. Analyses of samples collected using sediment traps deployed at 150 m revealed that members of diatoms, prymnesiophytes, and pelagophytes all contributed to material export out of the upper ocean. None of the phytoplankton groups displayed significant seasonality in gene abundances or fluxes over the period of observations. Our study confirms that diatoms are ubiquitous and diverse members of the euphotic zone phytoplankton assemblage in the NPSG, while prymnesiophytes and pelagophytes appear to capitalize on the relatively nutrient-enriched but low light conditions characteristic of the deeper euphotic zone waters. The combined use of molecular- and pigment-based tools demonstrated that despite persistently oligotrophic conditions chromophytic plankton are perennial contributors to upper ocean biomass and particle export in the NPSG.

© 2013 Elsevier Ltd. All rights reserved.

1. Introduction

Subtropical ocean gyres occupy ~40% of Earth's surface area and play a central role in global carbon cycling. The North Pacific Subtropical Gyre (NPSG) is among the largest of these open ocean habitats (Sverdrup et al., 1942; Karl, 1999). Persistent stratification of the upper ocean of the NPSG reduces wind-driven convective mixing, and limits vertical delivery of nutrients (Dore et al., 2002; Karl, 2002). Surface waters of the NPSG are characterized by low nutrient concentrations, deep penetration of photosynthetically available radiation, low plankton biomass, and dominance of plankton biomass by photosynthetic cyanobacteria such as *Prochlorococcus* and *Synechoccocus* (Campbell and Vaulot, 1993; Letelier et al., 1993; Andersen et al.,1996; Malmstrom et al., 2010).

Although much of the research on phytoplankton dynamics in the NPSG has emphasized the important role of picoplankton as contributors to productivity and biomass (Campbell and Vaulot, 1993; Karl et al., 2001; Church et al., 2006), nano- and micro-phytoplankton also play important roles in regulating ecological and biogeochemical dynamics in this ecosystem. Despite

* Corresponding author. Tel.: +1 808 956 8779.
E-mail address: mjchurch@hawaii.edu (M.J. Church).

0967-0645/$ - see front matter © 2013 Elsevier Ltd. All rights reserved.
http://dx.doi.org/10.1016/j.dsr2.2013.03.007

occurring at lower abundances than picoplankton, these larger phytoplankton can exhibit rapid growth, making them potentially important episodic contributors to phytoplankton biomass and productivity in the open sea (Li, 1993; Worden et al., 2004).

Over the course of nearly 20 years (1968–1985), microscopic evaluations of phytoplankton taxa larger than 5 μm collected in the northern regions of the NPSG (~28°N, 155°W) provided detailed information on vertical and time-variability in phytoplankton community structure (Venrick, 1982, 1988, 1990, 1992). These studies identified two vertically separated phytoplankton assemblages (Venrick, 1982): one assemblage of photosynthetic plankton that was largely restricted to the high-light, low-nutrient region of the upper euphotic zone, and another assemblage often associated with the deep chlorophyll maximum layer (DCML), where nutrient concentrations increase, but penetration of light becomes more variable and often limits phytoplankton growth (Venrick, 1982; Letelier et al., 2004; Li et al., 2011). More than 230 phytoplankton species were identified and listed as part of these early studies, including 101 diatom species and 47 species belonging to the prymnesiophytes (Venrick, 1982). In the summers of 1994 and 1996, Venrick (1997, 1999) compared phytoplankton species collected at Station ALOHA (22°45′N, 158°W) to those previously observed in the northern regions of the NPSG. These studies revealed that similar genera and species inhabited both of these open ocean locations, including flora associated with shallow and deeper euphotic zone waters (Venrick, 1997, 1999).

Research at Station ALOHA conducted as part of the Hawaii Ocean Time-series (HOT) program has also demonstrated that particle export and fluctuations in plankton biomass are partly controlled by episodic, seasonal, and interannual-scale variations in the diversity of eukaryotic phytoplankton (Letelier et al., 2000; Bidigare et al., 2009; Karl et al., 2012). High-performance liquid chromatography (HPLC) separation and analyses of selected algal pigments indicate that prymnesiophytes and pelagophytes can be major components of eukaryotic phytoplankton biomass (Letelier et al., 1993; Andersen et al., 1996; Karl et al., 2002; Bidigare et al., 2009). In a study focused on prymnesiophyte ecology at ALOHA, Cortés et al. (2001) identified upwards of 125 distinct species of coccolithophores, finding that abundances generally increased in the spring and fall. Scharek et al. (1999a) investigated the abundance of diatoms during 11 cruises (1994–1995) to Station ALOHA, finding that two lightly silicified diatom species (*Hemiaulus hauckii* and *Mastogloia woodiana*) increased in abundance in July 1994 within the well stratified mixed layer. Moreover, these diatoms were identified as key contributors to material export from the upper ocean to the deep sea (Scharek et al., 1999b; Karl et al., 2012).

The purpose of our study was to examine the variability in the population dynamics of three key groups of chromophytic phytoplankton at Station ALOHA: diatoms, prymnesiophytes, and pelagophytes. Changes in euphotic zone phytoplankton *rbcL* gene abundances and those caught in sediment traps (150 m depth) were evaluated from samples collected over ~2 year period on near-monthly HOT program cruises to Station ALOHA. Vertical and temporal variations in these phytoplankton assemblages were examined based on assessment of *rbcL* gene diversity and abundances together with analyses of selected algal pigments. Our results highlight temporal variability in the population structure of the eukaryotic algal assemblages in this oligotrophic environment.

2. Materials and methods

2.1. Upper ocean and sediment trap sampling and analyses

Sampling for this study was conducted on near-monthly HOT cruises to Station ALOHA over an approximately 2-year period (October 2007–December 2009). Samples were collected from 8 discrete depths in the upper ocean (5, 25, 45, 75, 100, 125, 150, and 175 m) using 12 l polyvinyl chloride bottles attached to a conductivity-temperature-depth (CTD) rosette sampler. Ten liters were subsampled into polyethylene carboys and pressure filtered onto 47 mm diameter 2 μm porosity polycarbonate filters for subsequent extraction of planktonic DNA. These filters were placed in microcentrifuge tubes containing 500 μl of a solution containing 1% sodium dodecyl sulfate solution and 0.1 M EDTA (pH 8.0). Tubes were flash frozen and stored at −80 °C.

Samples for subsequent extraction of DNA were also collected from particle interceptor traps (Knauer et al., 1979) deployed at 150 m depth for ~2.5 days during each cruise over a two year period (January 2008–December 2009). These traps were filled with a 0.2 μm filtered sodium-chloride seawater brine solution (50 g NaCl l^{-1} amended to surface seawater), and deployed on a free-drifting, surface tethered array. Upon recovery of the trap array, the overlying low-density seawater was removed by siphoning and the trap solution was pressure filtered onto 47 mm diameter 2 μm porosity polycarbonate filters and frozen in 500 μl of the same buffer previously described.

2.2. DNA extraction, PCR amplification, and sequence analyses

DNA was extracted from the filters using a combined cetyltrimenthylammonium bromide (CTAB)-chloroform method (Zhang and Lin, 2005). Briefly, in the shorebased laboratory, 10 μl of a 20 mg ml^{-1} proteinase K solution was added to each microcentrifuge tube containing the sample filters and preservation buffer and incubated for approximately 12 h at 55 °C. After this initial incubation, 165 μl of a 10% CTAB solution was added to each tube and the filters were incubated for an additional 10 min at 55 °C, followed by the addition of 600 μl of chloroform (99.8%, HPLC grade). Samples were vortexed for 1 min and centrifuged at room temperature (13,000 *g*) for 10 min, and the supernatants were purified using a Genomic DNA Clean & Concentrator kit (Zymo Research, Irvine, CA).

We utilized chloroplast form ID *rbcL* genes to examine phylogenetic relationships among chromophytic phytoplankton. The *rbcL* gene encodes the large subunit of ribulose-1,5-bisphosphate carboxylase oxygenase (RuBisCO), the enzyme catalyzing the initial step of carbon fixation in the Calvin–Benson cycle. The RuBisCO protein has several structural forms (Watson and Tabita, 1996), and these differences are reflected in variations in *rbcL* gene phylogeny (Tabita et al., 2007). Many eukaryotic algae and cyanobacteria possess a form of the RuBisCO enzyme termed form I, which includes at least four distinct taxonomic lineages termed forms IA, IB, IC and ID (Tabita, 1999). Previous studies have documented the utility of form ID genes for distinguishing phylogenetic relationships among chromophytic phytoplankton (Paul et al., 1999, 2000; Mann et al., 2001; Wawrik et al., 2002, 2003).

PCR-primers specific to form ID *rbcL* genes (forward primer, 5′-GATGATGARAAYATTAACTC-3′; reverse primer, 5′-ATTTGDCCA-CAGTGD ATACCA-3′, Paul et al., 2000) were used to amplify a 554-bp gene fragment from the DNA extracts obtained in this study. The PCR mix consisted of 2 μl plankton DNA extracts, 30 μl of nuclease free water, 5 μl of Ex Taq buffer (TaKaRa, Otsu, Japan), 4 μl of 2.5 mM dNTP mix, 4 μl of each 10 μM forward and reverse primers, and 1.5 U of ExTaq polymerase (TaKaRa). Total PCR reaction volumes were 50 μl. Thermal cycling conditions were: 3 min at 95 °C, followed by 40 cycles of 1 min at 95 °C, 1 min at 52 °C, and 1 min 30 s at 72 °C, with a final extension at 72 °C for 15 min. The resulting PCR products were visualized on an ethidium bromide-stained 1.2% agarose gel. PCR amplicons were excised and purified using the QIAquick Gel purification kit

Table 1
Oligonucleotide primers utilized for quantitative PCR analysis of selected form ID *rbcL* genes.

Targeted phylotypes	Forward primer (5′–3′)	Reverse primer (5′–3′)	qPCR efficiency (%)
Diatoms	5′-GATGATGARAAYATTAACTC-3′	5′-GTAAACTDGCCCADKNCATTTC-3′	85–92
Prymnesiophytes	5′-GGTTTCTACAACACTYTWYTWG-3′	5′-ATTTGDCCACAGTGDATACCA-3′	84–92
Pelagophytes	5′-CRACACWTTATTARAGACTAAG-3′	5′-ATTTGDCCACAGTGDATACCA-3′	85–95

(Qiagen, Valencia, CA). The purified PCR products were ligated into pGEM-T Easy Vectors and transformed in *Escherichia coli* JM109 competent cells following the manufacturer's instructions (Promega, Madison, WI). Plasmids containing the PCR amplified *rbcL* gene fragments were extracted and purified using QIAprep Spin Miniprep kit (Qiagen), prior to sequencing using an ABI 3100 Gene Analyzer (Applied Biosystems, Carlsbad, CA). Sequences were edited using BioEdit and the translated protein sequences were aligned and imported into ARB (Ludwig et al., 2004) for subsequent phylogenetic analyses. All sequences were submitted to GenBank (National Center for Biotechnology Information) and assigned accession numbers KC533892–KC534141.

2.3. Primer design and qPCR amplification

More than 350 marine phytoplankton form ID *rbcL* sequences obtained from GenBank (NCBI) and from our own environmental clone libraries were used to design and evaluate the specificity of quantitative PCR (qPCR) primers targeting phylotypes found at Station ALOHA. Three primer sets were developed to target form ID *rbcL* genes from clones phylogenetically clustering among diatoms, prymnesiophytes, and pelagophytes, respectively (Table 1). The abundances of *rbcL* genes from these major chromophyte taxa were estimated using qPCR, where qPCR reactions included: 12.5 μl 2X SybrGreen Master Mix (Applied Biosystems), 5.5 μl of nuclease free water, 2 μl each of 10 μM forward and reverse primers, 1 μl of 10 mg ml^{-1} Bovine Serum Albumin (BSA, BioLabs, Ipswich, MA) and 2 μl of DNA extract. Thermal cycling conditions for the qPCR reactions were: 94 °C for 15 min; 40 cycles of 15 s at 94 °C, 30 s at 48 °C, 35 s at 72 °C, followed by extension at 72 °C for 7 min. Melt curves were run between 44 °C and 95 °C with the resulting amplicon dissociation products detected at 1 °C intervals. Standards for the qPCR reactions consisted of serial 10-fold dilutions of plasmids containing targeted DNA fragments. qPCR reactions were run in duplicate for each environmental DNA sample and for each standard, and the mean of the replicate reactions were used. Specificities of the qPCR primers were evaluated by comparing the amplification cycle threshold between plasmids containing the intended target *rbcL* insert and those containing non-target form ID *rbcL* genes. In each case, the primer set specificity was tested using at least 8 non-target controls; for example, 4 plasmids containing PCR amplified *rbcL* genes derived from different types of pelagophytes and 4 plasmids containing PCR amplified *rbcL* genes derived from different types of prymnesiophytes were tested with the diatom primer set. No significant amplification after 40 cycles of PCR was found for these non-target controls. Comparison of the aligned sequences indicated that the selected primers contained less than 2 base-pair mismatches to the intended targets, while the non-target controls contained >2 base-pair differences to both the forward and reverse primers.

2.4. Upper ocean physical and biogeochemical measurements

The daily flux of photosynthetically active radiation (PAR; 400–700 nm) at the sea surface was measured on each HOT cruise using a LI-COR LI-1000 cosine collector. In addition, vertical profiles of PAR were conducted at approximately noon on each HOT cruise using a Profiling Reflectance Radiometer (PRR; Wetlabs, Philomath, OR). Vertical profiles of temperature, conductivity, and pressure were obtained using a SeaBird conductivity-temperature-depth (CTD) sampler described by Karl and Lukas (1996). High-sensitivity measurements of nitrate + nitrite (N + N) were determined as described by Dore and Karl (1996). Measurements of suspended and sediment trap particulate carbon (PC), particulate nitrogen (PN), and particulate phosphorus (PP) were determined as described in Karl et al. (1996) and Hebel and Karl (2001). Measurements of particulate silica (PSi) utilized the sodium bicarbonate dissolution time-course assay described in DeMaster (1981). Rates of ^{14}C-bicarbonate assimilation were determined in the upper 125 m using the protocols described in Letelier et al. (1996).

Table 2
Pigment algorithms used to estimate contribution to total Chl *a* by selected groups of chromophytic phytoplankton modified from Letelier et al. (1993). Pigments abbreviations are: 19′-hexanoyloxyfucoxanthin (19-hex), 19′-butanoyloxyfucoxantin (19-but). P represents the 19-hex to 19-but ratio in prymnesiophytes and C represents the 19-hex to 19-but ratio in pelagophytes.

Algal group	Equation
Diatoms	$[\text{Chl } a]_{\text{diatom}} = 0.8([\text{fucoxanthin}] - 0.14\ [\text{19-but}]_{\text{pel}})$
Prymnesiophytes	$[\text{Chl } a]_{\text{pry}} = 1.3[\text{19-hex}]_{\text{pry}}$
Pelagophytes	$[\text{Chl } a]_{\text{pel}} = 0.9[\text{19-but}]_{\text{pel}}$
	$[\text{hex}]_{\text{pry}} = (P/(P-C)) \times ([\text{19-hex}]_{\text{total}} - [\text{19-but}]_{\text{total}} \times C)$
	$[\text{but}]_{\text{pel}} = (P/(P-C)) \times ([\text{19-but}]_{\text{total}} - [\text{19-hex}]_{\text{total}}/P)$
	$P = [\text{19-hex}]_{\text{pry}}/[\text{19-but}]_{\text{pry}} = 65.44$
	$C = [\text{19-hex}]_{\text{pel}}/[\text{19-but}]_{\text{pel}} = 0.14$

Chl *a* and photosynthetic accessory pigments were measured by high-performance liquid chromatography (HPLC) according to the procedures described in Bidigare et al. (2005). We utilized several photosynthetic cartenoid pigments as diagnostic indicators of diatoms (fucoxanthin), prymnesiophytes (19′-hexanoyloxyfucoxanthin, abbreviated as 19-hex), and pelagophytes (19′-butanoyloxyfucoxanthin, abbreviated as 19-but). We estimated the contributions of these phytoplankton taxa to total Chl *a* in the lower regions of the euphotic zone (75–125 m) using a modified pigment algorithm (Table 2) based on Letelier et al. (1993). Specifically, the 19-hex to 19-but ratio for prymnesiophytes was re-estimated based on four cultures of prymnesiophytes (Jeffrey and Wright, 1994). The Chl *a* contributed by diatoms was calculated from fucoxanthin concentrations and 19-but concentrations (Mackey et al., 1996).

3. Results

3.1. Upper ocean biogeochemical characteristics

Consistent with the well-resolved climatology at Station ALOHA, the euphotic zone during this period appeared to generally form two vertically segregated habitats: our 3 shallow sampling depths (5, 25, and 45 m) corresponded to a high-light, low-nutrient environ that supported the majority of primary production, while samples collected between 75 and 125 m were

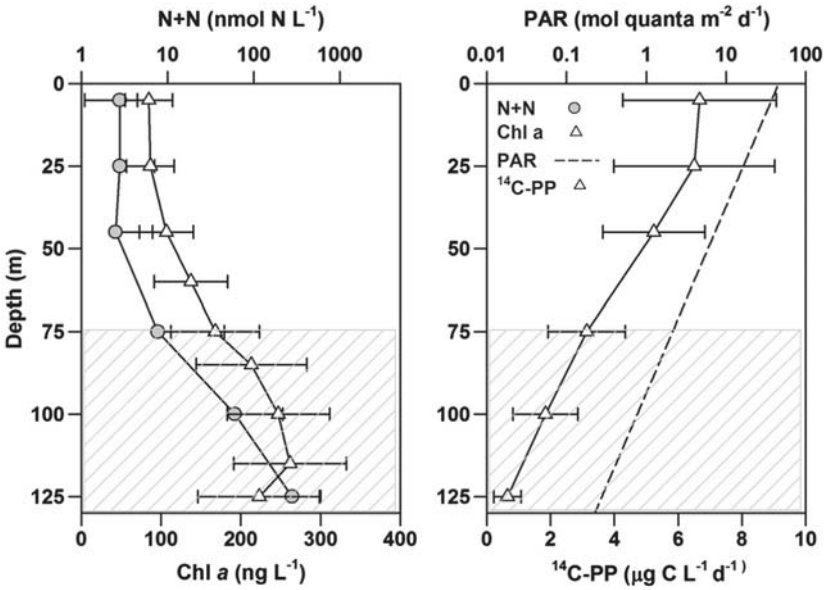


Fig. 1. Time-averaged concentrations of Chl *a* and nitrate+nitrite (N+N) (left panel) and rates of ^{14}C-based primary production and daily flux of photosynthetically active radiation (PAR; right panel) in the upper ocean (0–125 m) at Station ALOHA. Error bars depict standard deviations of mean concentrations and rates. Hashed boxes depict the vertical separation between upper (0–45 m) and lower (75–125 m) regions of the euphotic zone.

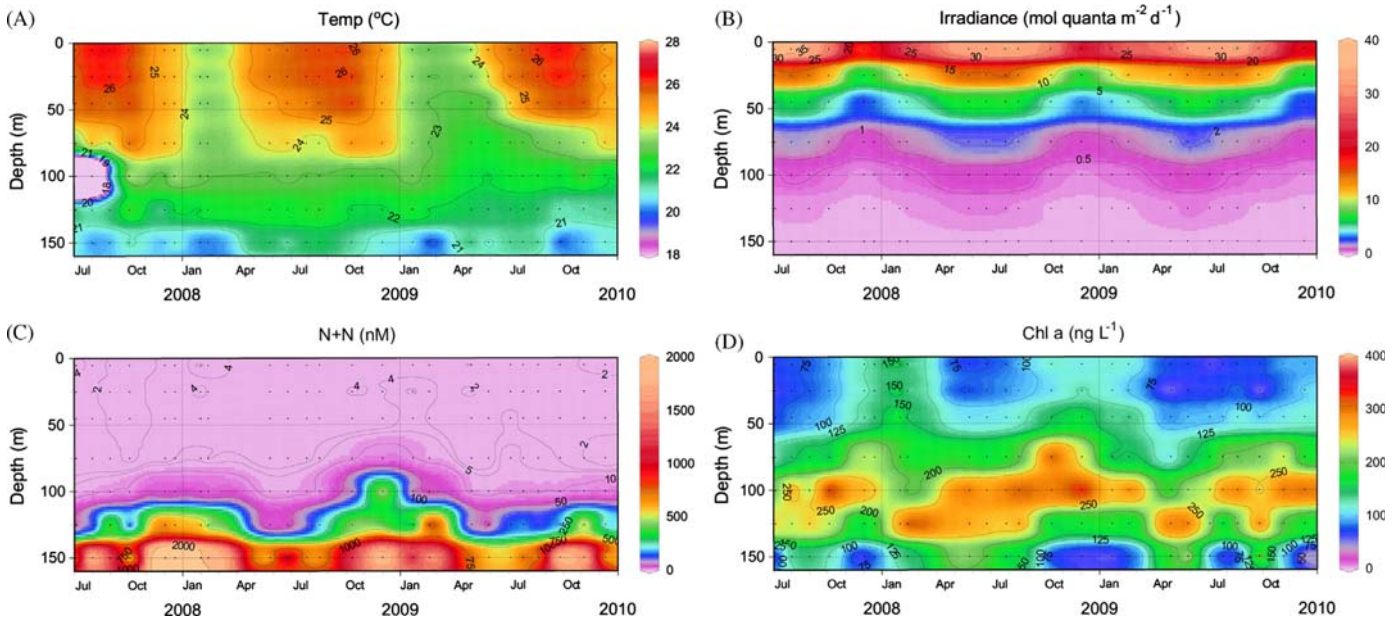


Fig. 2. Contour plots of temperature (A), photosynthetically active radiation (PAR) (B), nitrate+nitrite (N+N) concentrations (C), and Chl *a* (D) in the upper 150 m at Station ALOHA during this study (October 2007–December 2009).

typical of the low-light, nutrient-enriched lower euphotic zone that included the deep chlorophyll maximum layer (DCML; Fig. 1). On average, concentrations of N+N were consistently low (<4 nM) in the well-lit regions of the euphotic zone (0–45 m), with nutrient concentrations increasing sharply below 75 m (Fig. 1). Concentrations of Chl *a* were low in the upper 45 m (averaging 103 ± 35 ng L^{-1}), increasing through the mid-euphotic zone (75–125 m), before declining again toward the base of the euphotic zone where light fluxes decreased to $<1\%$ of the surface irradiance (Fig. 1). Rates of ^{14}C-based primary production were elevated in the upper euphotic zone, ranging between 2.5 and 10.8 µg C L^{-1} d^{-1}, with production decreasing with depth (Fig. 1).

Over the period of this study, sea-surface temperatures varied between 22.9 °C and 26.6 °C with euphotic zone temperatures relatively homogenous during the winter (varying <2 °C), with the upper ocean warming and becoming more stratified during the summer and fall months (Fig. 2). PAR at the sea surface varied approximately 4-fold (ranging 17 to 47 mol quanta m^{-2} d^{-1}), with downwelling subsurface irradiance varying as much as 12-fold (0.03–0.37 mol quanta m^{-2} d^{-1}) at our deepest sampling depth (125 m). Deepening of isolumes in the late spring and early summer coincided with periods of lower concentrations of N+N in the dimly lit region of the euphotic zone, with increasing N+N concentrations during wintertime periods when isolumes shoaled upwards (Fig. 2). Concentrations of Chl *a* in the upper euphotic

zone (0–45 m) ranged between 42 and 215 ng L^{-1} (averaging 103 ng L^{-1}), while concentrations in the lower euphotic zone (75–125 m) varied between 81 and 374 ng L^{-1} (averaging 234 ng L^{-1}) (Fig. 2). Chl *a* concentrations tended to be greatest between 100 and 125 m, where light decreased to < 2% of the surface flux. The DCML generally deepened in the late spring and early summer, shoaling upward in the late fall and winter consistent with seasonal variations in light availability (Letelier et al., 2004; Fig. 2).

3.2. *rbcL* gene clone libraries

PCR amplified chromophytic algal chloroplast *rbcL* gene sequences (n=238) were obtained from samples collected throughout the euphotic zone (0–150 m) and upper ocean sediment traps (150 m). These environmental *rbcL* sequences clustered with 4 major form ID chromophytic algal *rbcL* gene clades, including genera of diatoms, pelagophytes, prymnesiophytes, and dinoflagellates (Fig. 3). One hundred forty of these *rbcL* gene sequences clustered (89–96% identity) among more than 12 known diatom genera (Fig. 3); the majority of these sequences phylogenetically grouped among diatom *rbcL* genes belonging to the genera *Hemiaulus, Chaetoceros*, *Corethron*, *Pseudonitzschia*, and *Thalassiosira* (Fig. 3). Seventy-five *rbcL* gene sequences clustered (88–100% identity) among seven known genera of prymnesiophytes, including *Emiliania, Phaeocystis, Umbilicosphaera, Calyptrosphaera, Helicosphaera, Chrysochromulina*, and *Gephyrocapsa*. Sequences most closely related (91–100%) to *Emiliania* were retrieved exclusively from samples collected in the upper euphotic zone (0–45 m), while sequences phylogenetically clustering among *Chrysochromulina* were all retrieved from samples collected in the mid to lower euphotic zone (75–125 m). In total, 71 sequences clustered (87–99% identity) among pelagophytes belonging to the genera: *Pelagomonas*, *Pelagococcus*, and *Aureococcus*. Sequences most similar to *rbcL* genes belonging to *Pelagomonas* were exclusively retrieved from the lower euphotic zone (75–125 m) and from sediment traps, while sequences clustering with *Aureococcus* were only retrieved from samples collected in the upper euphotic zone waters (0–45 m) and in sediment traps (Fig. 3).

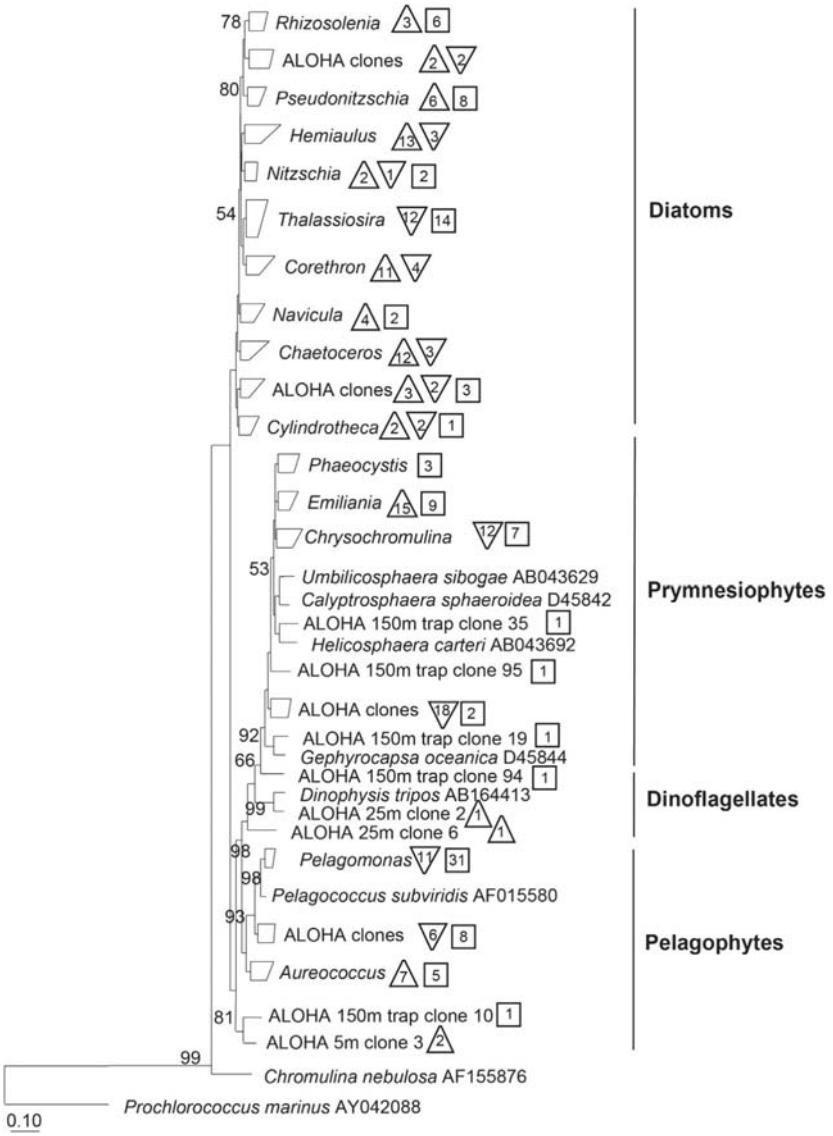


Fig. 3. Neighbor-joining phylogenetic tree of chromophyte algae form ID *rbcL* gene sequences. Sequences retrieved from the upper ocean (0–45 m), lower euphotic zone (75–150 m), and floating sediment traps (150 m) at Station ALOHA depicted by triangles, upside down triangles, and squares, respectively. Numbers inside each symbol indicate the number of clones sequenced. Polygons represent grouping of *rbcL* sequences sharing > 85% identity. Bootstrap percentages > 50% are indicated at the tree nodes; tree was rooted using the form 1A *rbcL* gene sequence of *Prochlorococcus marinus* (CCMP1375).

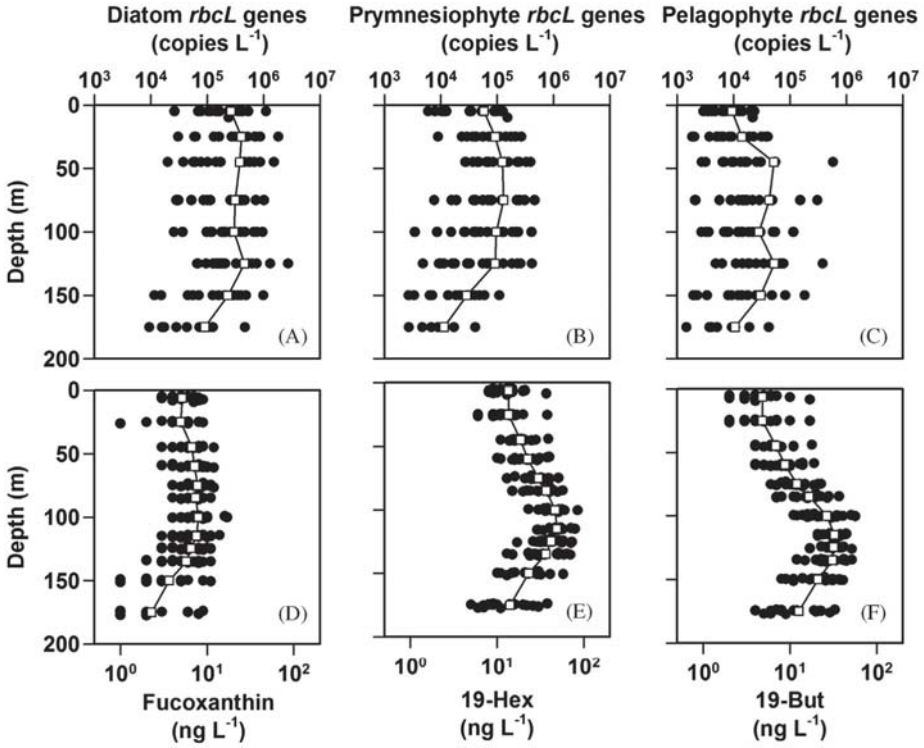


Fig. 4. Depth profiles of *rbcL* gene abundances of diatoms (A), prymnesiophytes (B), and pelagophytes (C) at Station ALOHA. Also depicted are concentrations of fucoxanthin (D), 19′-hexanoyloxyfucoxanthin concentration (E), and 19′-butanoyloxyfucoxanthin (F) at Station ALOHA. Open squares represent time-averaged gene abundances and pigment concentrations during the study.

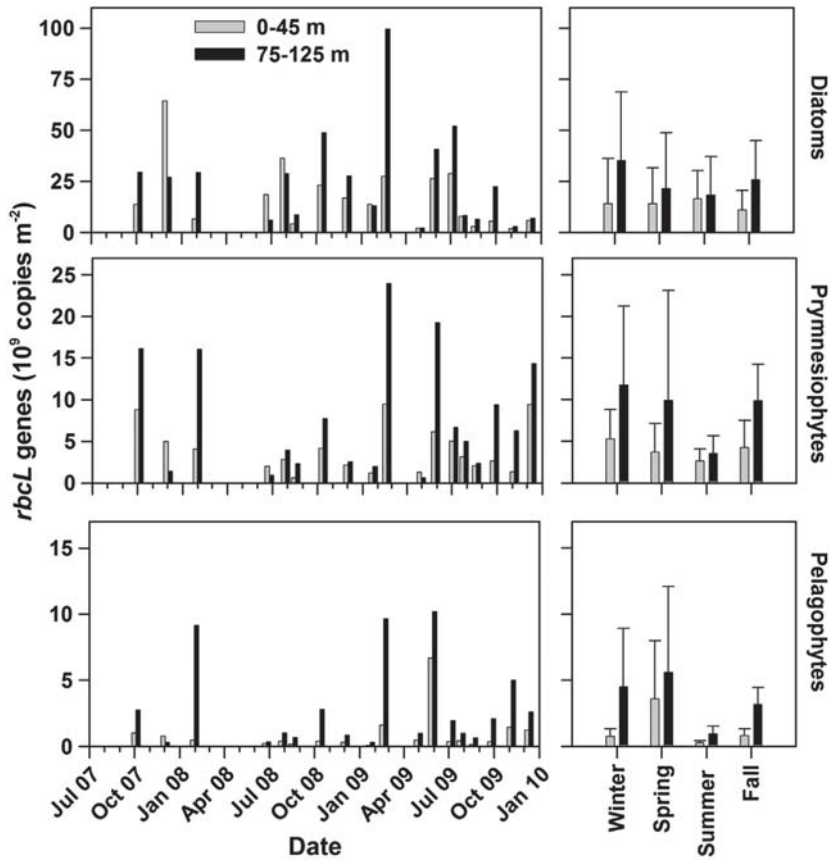


Fig. 5. Temporal variability in depth-integrated *rbcL* gene abundances at Station ALOHA. Gene abundances of diatoms, prymnesiophytes, and pelagophytes in the upper euphotic zone (0–45 m, gray bars) and in the lower euphotic zone (75–125 m, black bars) during the study period. Seasonal binning as described in Table 3; error bars indicate standard deviations of the seasonal means.

A total of 107 *rbcL* gene sequences were retrieved from samples collected using upper ocean sediment traps, with 45 of these sequences clustering with *rbcL* gene sequences from pelagophytes. The majority (31) of these pelagophyte sequences were most closely (91–99%) related to the *rbcL* gene sequence of *Pelagomonas calceolate*, a 2–4 μm diameter flagellated cell (Andersen et al., 1993; Daugbjerg and Andersen, 1997). An additional 36 sequences derived from sediment trap samples were phylogenetically related to diatom *rbcL* gene sequences, including diatoms belong to the genera: *Thalassiosira*, *Rhizosolenia*, *Nitzschia*, *Pseudonitzschia*, and *Cylindrotheca*. Finally, 26 sequences retrieved from the sediment trap samples clustered among *rbcL* gene sequences of prymnesiophytes; the majority (16) of these sequences clustered with *Emiliania huxleyi* and *Chrysochromulina* spp.

3.3. Vertical and temporal variability in rbcL gene abundances

Analyses of the abundances of form ID *rbcL* genes provided insight into the vertical and temporal variability associated with the abundances of diatoms, pelagophytes, and prymnesiophytes. Throughout the euphotic zone diatoms were often the most abundant taxon examined (Fig. 4) with *rbcL* gene abundances ranging between 4×10^3 and 2×10^6 gene copies L^{-1}. Gene abundances of prymnesiophytes ranged between 3×10^3 and 4×10^5 gene copies L^{-1}, with abundances often increasing into the lower regions (75–125 m) of the euphotic zone (Fig. 4). Abundances of pelagophytes were generally the lowest of the taxa examined with *rbcL* gene abundances ranging between 2×10^2 and 6×10^5 gene copies L^{-1} (Fig. 4).

Depth integration of the gene abundances revealed that diatoms dominated the *rbcL* gene inventories in both the upper (0–45 m) and lower (75–125 m) regions of the euphotic zone (Fig. 5). The *rbcL* gene inventories of all three taxa were highly variable in time in both the upper and lower euphotic zone. There were no significant differences in diatom *rbcL* gene inventories between the upper and lower euphotic zone (One-way ANOVA, $P>0.05$); however, diatom *rbcL* gene abundances were significantly greater than abundances of pelagophytes and prymnesiophytes throughout the upper and lower regions of the euphotic zone (One-way ANOVA, $P<0.05$). Gene inventories of both the pelagophytes and prymnesiophytes were significantly greater (One-way ANOVA, $P<0.05$) in the lower euphotic zone than in the well-lit regions of the upper ocean. None of the taxa examined demonstrated statistically significant seasonality (one-way ANOVA, $P>0.05$) in either the upper or lower euphotic zone. However, throughout the study period, *rbcL* gene abundances of prymnesiophytes and pelagophytes were positively correlated in

Table 3
Seasonally averaged ± standard deviation of total Chl *a* (T Chl *a*) stocks in the lower euphotic zone (75–125 m) and the derived contributions to total Chl *a* by prymnesiophytes (Chl a_{pry}), pelagophytes (Chl a_{pel}), and diatoms (Chl a_{dia}) based on application of the modified pigment algorithm of Letelier et al. (1993). Also depicted are the derived relative contributions (as % of total Chl *a*) by the selected algal taxa (Chl a_{pry} %, Chl a_{pel} %, and Chl a_{dia} %).

Season (months)	T Chl *a* (μg m^{-2})	Chl a_{pry} (μg m^{-2})	Chl a_{pry} %	Chl a_{pel} (μg m^{-2})	Chl a_{pel} %	Chl a_{dia} (μg m^{-2})	Chl a_{dia} %
Winter (Jan–Feb, *n*=4)	10564 ± 735	2425 ± 606	23 ± 4	997 ± 397	9 ± 3	210 ± 40	2 ± 0.3
Spring (Mar–May, *n*=3)	11891 ± 2617	2458 ± 609	21 ± 3	843 ± 165	7 ± 1	187 ± 66	2 ± 1
Summer (Jun–Aug, *n*=6)	12424 ± 1505	2556 ± 277	21 ± 1	963 ± 212	8 ± 1	158 ± 85	1 ± 1
Fall (Sep–Dec, *n*=8)	13119 ± 922	2627 ± 159	20 ± 1	1297 ± 257	10 ± 2	155 ± 108	1 ± 1

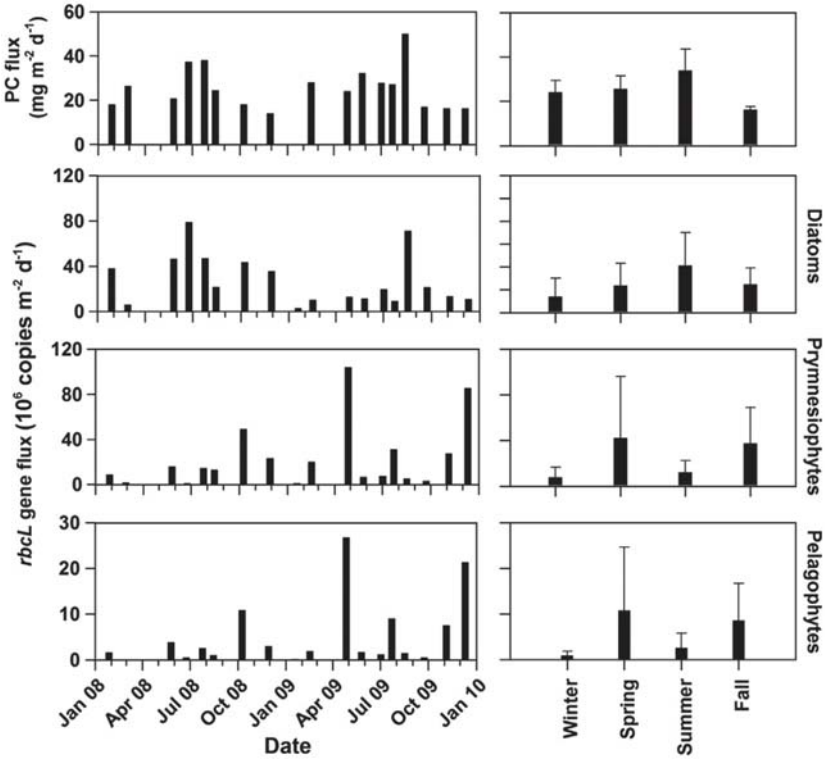


Fig. 6. Temporal variability in particulate material fluxes at 150 m at Station ALOHA. Depicted are particulate carbon, diatom *rbcL* gene, prymnesiophyte *rbcL* gene and pelagophyte *rbcL* gene fluxes. Seasonal binning as described in Table 3; error bars indicate standard deviations of the seasonal means.

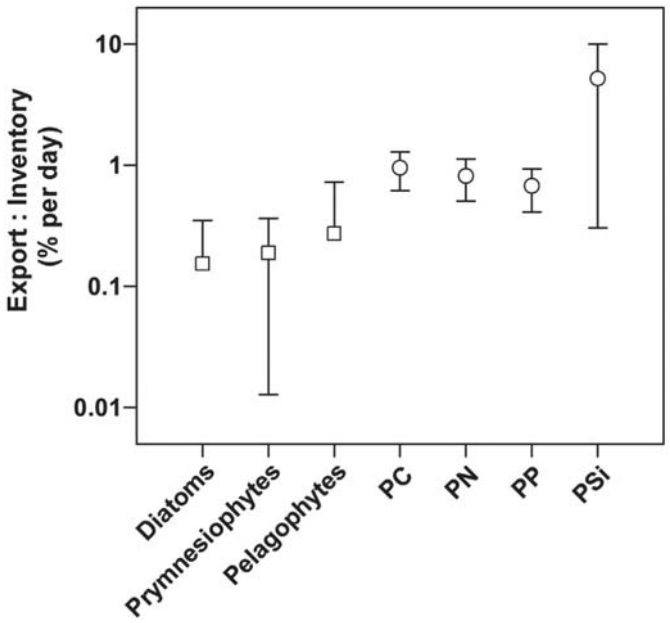


Fig. 7. Mean proportion of export to standing inventories (expressed as % per day) for three major *rbcL* phylotypes (squares) examined in this study and for bulk particulate carbon, nitrogen, phosphorus, and silica (PC, PN, PP, and PSi, respectively). Symbols depict mean of the ratios of export to inventories; error bars depict one standard deviation of the mean proportions. Export flux measured from upper ocean (150 m) sediment traps while inventories computed based on depth integration (0–125 m) of measured gene abundances or particulate matter concentrations.

time throughout the lower euphotic zone (least-square linear regression, $R^2=0.71$, $P<0.001$).

3.4. Vertical and temporal variability in accessory pigments

Concentrations of fucoxanthin, an accessory pigment produced by diatoms, varied ~10-fold over the study without clear vertical structure (Fig. 4). Concentrations of 19-hex and 19-but were generally low in the upper euphotic zone, and increased with depth so that concentrations of both pigments tended to be greatest in the DCML (Fig. 4). In the lower euphotic zone, concentrations of 19-hex and 19-but generally increased during the winter and late spring. Because of potential effects of seasonal photoadaptation in the well-lit region of the upper euphotic zone (0–45 m) we restricted the pigment-based estimation of taxonomic contributions of diatoms, prymnesiophytes, and pelagophytes to total Chl *a* concentrations to the low light region (75–125 m). The use of modified pigment algorithm described in Letelier et al. (1993) suggested that on average these 3 groups of chromophytic algae contributed 25–45% of the measured Chl *a* concentrations in the lower euphotic zone, with prymnesiophytes contributing 21% ($\pm$2%), pelagophytes 9% ($\pm$2%), and diatoms 2% ($\pm$1%) respectively (Table 3). A significant positive relationship was observed between Chl *a* contributed by prymnesiophytes and the contribution of pelagophytes (least-square linear regression, $R^2=0.42$, $P<0.01$) consistent with the positive correlation found between the *rbcL* gene abundances of prymnesiophytes and pelagophytes in the lower euphotic zone. Moreover, there was a significant positive relationship between Chl *a* and the derived contribution of prymnesiophytes to Chl *a* (least-square linear regression, $r^2=0.48$, $P<0.001$). There were no significant (one-way ANOVA, $P>0.05$) seasonal patterns in the contributions of these three phytoplankton taxa to Chl *a* in the lower euphotic zone (Table 3).

3.5. Export of rbcL genes out of the euphotic zone

We also examined temporal variability in chromophyte phytoplankton export based on qPCR amplification of selected form ID *rbcL* genes associated with sinking particulate material. Diatom *rbcL* gene fluxes fluctuated as much as 29-fold (3×10^6–8×10^7 gene copies $m^{-2}\,d^{-1}$) over the observation period (Fig. 6), while export of prymnesiophyte and pelagophyte *rbcL* genes varied 128-fold and 429-fold, respectively. Gene fluxes associated with diatoms were significantly greater than those of prymnesiophytes and pelagophytes (One-way ANOVA, $P<0.05$). None of the phylotypes demonstrated significant seasonal variability in *rbcL* gene export (Fig. 6, One-way ANOVA, $P>0.05$).

We also compared differences among the taxa in the proportion of *rbcL* genes exported relative to the depth integrated (0–125 m) standing stocks (expressed as % per day). Excluding one anomalously large prymnesiophyte export event (April 2009), the average gene flux to standing stock proportions for diatoms, prymnesiophytes, and pelagophytes were $0.15\pm0.20\%$, $0.19\pm0.18\%$, and $0.27\pm0.46\%$ per day, respectively (Fig. 7). Hence, although diatoms were the dominant contributors to measured *rbcL* gene fluxes, the export to stand stock ratio was generally similar among the taxa examined. In comparison, the percent export to standing stock ratio for bulk PC, PN, PP, and PSi pools averaged $0.95\pm0.33\%$, 0.81 ± 0.31, 0.67 ± 0.26, and $5.1\pm4.9\%$ and per day, respectively (Fig. 7). These data suggest that in comparison to PC, PN, and PP, export of PSi appears disproportionately large relative to its euphotic zone inventory. Notably, the *rbcL* gene export to inventory ratio for all three taxa was at least four-fold lower than this ratio for the bulk PC, PN, and PP pools, and more than an order of magnitude lower than the bulk PSi pool (Fig. 7).

4. Discussion

Our results revealed that despite persistently oligotrophic conditions, the euphotic zone of this ecosystem harbors a diverse assemblage of chromophytes. Among the three major phytoplankton groups examined diatoms were often the most abundant, with depth-integrated *rbcL* gene inventories in both the upper and lower euphotic zone frequently 4–5-fold greater than those of the prymnesiophytes and pelagophytes. Moreover, results of PCR amplifying, cloning, and sequencing of diatom *rbcL* genes revealed diverse groups of diatoms inhabiting this persistently oligotrophic ecosystem.

Given our interests in examining temporal and vertical variability in phytoplankton assemblages in the NPSG, we utilized chloroplast *rbcL* genes as molecular biomarkers to specifically target photosynthetic eukaryotes. By examining diversity in form ID *rbcL* genes, we developed and applied group-specific qPCR primers to obtain information on the gene abundances of three groups of chromophytic algae. Several previous studies have applied reverse-transcription PCR (RT-qPCR) assays to examine temporal and spatial variability in patterns of *rbcL* gene transcription by diatoms, haptophytes, and unicellular cyanobacteria belonging to the genera *Prochlorococcus* and *Synechococcus* (Wawrik et al., 2002, 2003; John et al., 2007). To our knowledge, the present study is the first study to examine time-variability in *rbcL* gene abundances among several major groups of phytoplankton in the open sea. Cloning and sequencing of PCR amplified *rbcL* genes from the euphotic zone at Station ALOHA revealed numerous sequences closely related to diatoms, prymnesiophytes, dinoflagellates, and pelagophytes. Notably, nearly half (125 out of 288 total) of the clones sequenced as part of this study clustered among diverse lineages of diatoms, confirming that these organisms constitute important components of the

eukaryotic plankton assemblage in this oligotrophic habitat. Such results were further supported by our qPCR amplification results indicating that diatom *rbcL* genes were often the most abundant of the groups examined in both the upper and lower euphotic zone.

The prevalence of diatom *rbcL* genes retrieved in the present study is consistent with previous studies in the NPSG reporting diverse lineages of diatoms throughout the euphotic zone. Venrick (1982, 1997) identified two vertically segregated groups of diatoms, including those best adapted to high light low nutrient conditions, and those most abundant in the low light nutrient-enriched regions of the euphotic zone. In our study, the *rbcL* gene abundances of diatoms in both the upper and lower regions of euphotic zone tended to be similar, suggesting the diverse assemblage of diatoms in this ecosystem possesses widely varying physiological capabilities, including those adapted to growth under conditions of high light but low nutrient supply, with others adapted to persistently low light but relatively enriched concentrations of nutrients. Previous investigations into diatom population dynamics in this ecosystem have highlighted episodic occurrences of blooms of selected genera of diatoms in the well-lit regions of the upper euphotic zone (Scharek et al., 1999a; Fong et al., 2008; Dore et al., 2008; Brzezinski et al., 2011). Such blooms frequently occur during the summer months and are large enough to be visible by Earth-orbiting satellites (White et al., 2007; Dore et al., 2008). Moreover, these blooms coincide with periods when rates of N_2 fixation increase and the abundances of cyanobacteria belonging to the genera *Richelia*, *Calothrix*, and *Trichodesmium* are elevated (Church et al., 2009). Based on the time-varying concentrations of Chl *a*, fucoxanthin, and diatom gene abundances in the present study, it appears we did not sample such a bloom during the present study. Although previous studies have highlighted time-variable diatom population dynamics throughout the upper ocean, our study revealed that diatom population dynamics in the lower euphotic zone, below the depths detectable by satellites, can also be highly variable. We found no evidence of seasonality associated with diatom *rbcL* genes recovered from sediment traps, results that appear contradictory to previously described seasonality in diatom-derived driven flux of organic matter to the deep sea at Station ALOHA (Karl et al., 2012). However, our study relied on collection of sinking particles using particle interceptor traps, which are deployed for ~3 days on each monthly HOT cruise (Karl et al., 1996); in contrast, observations of summertime diatom-driven export of organic matter have relied on deep ocean, bottom-moored traps that continuously collect sinking particles throughout the year (Dore et al., 2008; Karl et al., 2012). Hence, we suspect part of the difference between our findings and these previous studies reflects undersampling in time by the upper ocean sediment traps utilized in our study.

Through modification and application of a previously developed pigment algorithm (Letelier et al., 1993) we evaluated the contributions of the chromophytic phytoplankton to total Chl *a* in the lower euphotic zone. The analysis was restricted to the lower euphotic zone to minimize variations in the pigment to Chl *a* ratios resulting from seasonal-scale photoadaptation occuring in the well lit region of the upper euphotic zone (0–45 m). Results from this model suggest that lineages of prymnesiophytes, pelagophytes, and to a lesser extent diatoms contributed on average 21%, 9%, and 2%, respectively to the total Chl *a* in the lower euphotic zone. Similar results were reported by Letelier et al. (1993) using data collected between 1989 and 1991. The complementary molecular and pigment-based approaches utilized in the current study emphasize the relatively large temporal variability underlying population dynamics associated with diatoms, prymnesiophytes, and pelagophytes in this ecosystem. However, these two approaches also highlight one important discrepancy: based on the pigment model diatoms were the lowest contributors to total Chl *a* in the lower euphotic zone, despite often dominating the *rbcL* gene abundances in both the upper and lower euphotic zone. The observed differences in vertical distributions between the *rbcL* gene abundances and related accessory pigments could derive from several factors, including: light/depth-dependent variations in amount of accessory pigments per cell, or variations in *rbcL* gene copies per cell for the different taxa. Moreover, the pigment-based model results rely on accessory pigment:Chl *a* ratios derived from relatively few cultured species in each taxa, and may not accurately describe the flexibility in this ratio among the diverse phytoplankton taxa found in this environment.

Pelagophytes and prymnesiophytes have been shown to be substantial contributors to phytoplankton biomass and productivity in various temperate, subtropical, and tropical regions of the open sea including the subarctic North Pacific (Obayashi et al., 2001; Suzuki et al., 2002), South Pacific Ocean (DiTullio et al., 2003), the Sargasso Sea (Cuvelier et al., 2010), Indian Ocean (Not et al., 2008), Mediterranean Sea (Barlow et al., 1997; Marty et al., 2002), and the Arabian Sea (Barlow et al., 1999). In the North Atlantic Barlow et al. (1993) estimated prymnesiophytes contributed 20–40% of the Chl *a*, with uncultivated members of the prymnesiophytes estimated to account for ~25% of the primary production in this ecosystem (Jardillier et al., 2010). Claustre and Marty (1995) estimated that pelagophytes and prymnesiophytes together comprised a large fraction of phytoplankton biomass in the lower euphotic zone of the tropical North Atlantic (21°N, 31°W) during both the spring and fall. In the near-surface waters of the Sargasso Sea, primary production by uncultivated groups of prymnesiophytes has been estimated to equal that of *Prochlorococcus* (Cuvelier et al., 2010). In the equatorial Pacific Ocean, Bidigare and Ondrusek (1996) estimated the contributions of these two phytoplankton taxa to total Chl *a*, finding prymnesiophytes and pelagophytes comprised 30–40% and 10–20% of the total Chl *a*, respectively, during two survey cruises in summer and winter. A recent metagenomic study by Worden et al. (2012) highlighted the global distribution of a pelagophyte whose *rbcL* gene sequence was 99% similar to *Pelagomonas calceolate*.

In a study comparing HPLC pigment and electron microscopy-derived determinations of phytoplankton community structure in the Sargasso Sea and the NPSG, Andersen et al. (1996) concluded that prynmesiophytes and pelagophytes were among the most abundant eukaryotic phytoplankton, contributing 30–60% to total euphotic zone Chl *a*. In the present study we found that *rbcL* gene abundances of pelagophytes and prynmesiophytes increased in the lower regions of the euphotic zone, highlighting a potentially important role for these organisms in controlling variability in Chl *a* concentrations in the DCML. Moreover, the temporal co-variance between both the accessory pigments (19-hex and 19-but) and *rbcL* gene abundances of prymnesiophytes and pelagophytes in the low light regions of the euphotic zone hints that these two groups of phytoplankton may respond similarly to time-varying environmental forcing (i.e. nutrients or light), and that top-down processes (i.e. predation, viruses) controlling the population sizes of these broad groups of organisms may also be temporally synchronized.

The frequent predominance of prymnesiophytes and pelagophytes in the lower euphotic zone, near the top of the nutricline, suggests that these phytoplankton taxa are physiologically adapted to low light, nutrient-enriched regions of the water. We observed sporadic increases in the gene abundances of these taxa, hinting that population dynamics associated with prymnesiophytes and pelagophytes at Station ALOHA may be tuned to high frequency, stochastic changes in nutrient supply occurring in the lower euphotic zone. Mesoscale forcing is a predominant control on habitat variability in the lower euphotic zone at ALOHA (Johnson et al., 2010), and satellite-derived sea surface height

anomalies (SSHa) in the vicinity of ALOHA appear reasonable predictors of vertical variability in isopycnal surfaces in the lower euphotic zone (Church et al., 2009). In the present study, gene abundances of diatoms, prymnesiophytes, and pelagophytes in the lower euphotic zone all peaked during periods of negative SSHa, indicative of uplift of isopycnal surfaces. Although there were no significant relationships between SSHa and the abundances of any of the phytoplankton taxa examined in this study (least squares linear regressions, $P > 0.05$), such results are not surprising given the spatiotemporal complexity associated with biological responses to mesoscale variability in the ocean.

Recent molecular-based approaches to phytoplankton dynamics at the Bermuda Atlantic Time-series Study (BATS) in the Sargasso Sea revealed seasonal succession patterns among members of the Prasinophyceae, Prymnesiophyceae, Pelagophyceae, Chrysophyceae, Cryptophycae, and Bacillariophyceae, with members of the prynmesiophytes, pelagophytes/chrysophytes, and prasinophytes all increasing in abundance during the period of deep winter mixing (Treusch et al., 2011). The lack of seasonality exhibited by the chromophytic algae examined in the present study is consistent with the overall weak seasonal forcing of the upper ocean habitat at ALOHA compared to BATS. While the upper ocean at BATS undergoes periods of relatively deep convective mixing (occasionally exceeding 300 m; Steinberg et al., 2001), the upper ocean at ALOHA exhibits only weak seasonality in mixing (mixed layer depths rarely exceed 110 m; Karl and Lukas, 1996). However, we observed large subseasonal scale variations in the abundances of all three phytoplankton taxa examined. While seasonal forcing of the epipelagic habitat would be expected to exert important control on plankton abundances at BATS, phytoplankton diversity, productivity, and biomass at ALOHA have all been shown sensitive to episodic or event-scale, near-surface perturbations such as those associated with submesoscale to mesoscale physical forcing (Letelier et al., 2000; Sakamoto et al., 2004; Church et al., 2009).

Chromophytic algal *rbcL* gene clone libraries from sediment trap samples revealed a large number of presumed pelagophyte *rbcL* genes associated with sinking particles, suggesting these small phytoplankton taxa might play a role in particle export in the oligotrophic open ocean. Such results support recent modeling studies based in the equatorial Pacific that suggest the export of picophytoplankton could be proportional to their productivity (Richardson and Jackson, 2007). In the subtropical North Atlantic, where seasonal changes in the upper ocean habitat are more pronounced, Amacher et al. (2009) compared 18S rRNA gene clone libraries from suspended particles to clone libraries constructed from sinking particulate flux caught in sediment traps and found that diatoms were major contributors to suspended particulate material, while Radiolarians and Alveolates appeared to dominate sediment trap clones. Although our results reveal that small nanoplankton can contribute to particle export at Station ALOHA, we do not know the mechanisms underlying these observations. In particular, it remains unclear whether the presence of these genes derives from repackaging of cells in fecal pellets, sinking of aggregates, or slow sinking by nanophytoplankton cells.

Although diatoms tended to dominate the downward flux of *rbcL* genes (among the three taxa examined), the relatively high standing stock of diatom *rbcL* genes resulted in a similar proportion of export relative to the euphotic zone inventory as that observed for the prymnesiophytes and pelagophytes. Comparison of the export to stand stock ratios for the different *rbcL* phylotypes to these ratios for bulk pools of PC, PN, PP, and PSi reveals very a low proportion of *rbcL* genes are exported from the upper ocean. The percent export of *rbcL* genes relative to the standing stock averaged ~0.2% per day for all the phytoplankton taxa; in comparison, these ratios averaged ~0.8% per day for the bulk PC, PN, and PP pools, and ~5% per day for the bulk PSi pools. Such analyses might suggest that these three broad taxa of phytoplankton are relatively minor contributors to export in this ecosystem; alternatively, these results might reflect rapid upper ocean turnover of cellular nucleic acid pools (and hence low proportional export) relative to bulk pools of PC, PN, PP, and PSi. The selective removal of nucleic acids from sinking particles would be expected in this oligotrophic habitat where nitrogen and phosphorus rich organic compounds are likely rapidly recycled in the upper ocean and hence contribute relatively little to the bulk particulate matter pools. Our results suggest the need for caution when attributing export of particulate material to specific organisms based on nucleic acid based methodologies. The preservation of nucleic acids in particulate matter depends on a complex suite of factors, including whether the organisms are still alive, factors controlling rates of organic matter remineralization, zooplankton feeding strategies, sinking rates of particles, and the composition of the organisms contributing to particle flux.

5. Conclusions

By examining temporal and spatial variability associated with three major groups of phytoplankton in the NPSG, this study has identified several ecologically and biogeochemically interesting features of this ecosystem. In particular, the finding that diatoms dominated *rbcL* gene abundances in both the well-lit, nutrient-poor and dimly-lit, nutrient-enriched regions of the euphotic zone suggests these diverse assemblages of organisms have evolved to capitalize on the vertically stratified habitat conditions found in the central ocean gyres. In contrast, our results suggest that both pelagophytes and prymnesiophytes occupy more specialized niches in this system, with abundances of both groups of organisms greater in the lower regions of the euphotic zone. In addition, we observed high month-to-month variability associated with all three groups of phytoplankton, suggesting these organisms could be responsive to high frequency physical perturbations superimposed over more subtle seasonal scale changes to the euphotic zone habitat.

Acknowledgments

We thank the HOT program scientists and staff, and the crew members of R/V *Kilo Moana* and R/V *Ka'imikai-O-Kanaloa* for support in the field and in the laboratory. We also acknowledge helpful comments from G.F. Steward and A.R. Sherwood. Three anonymous reviewers provided feedback that improved the manuscript. This work was supported by U.S. National Science Foundation with grants to the HOT program (OCE09-26766) and the Center for Microbial Oceanography: Research and Education (C-MORE; EF04-24599), and by the Gordon and Betty Moore Foundation (to D.M.K.).

References

Andersen, R.A., Saunders, G.W., Paskind, M.P., Sexton, J., 1993. Ultrastructure and 18S rRNA gene sequence for *Pelagomonas calceolate* gen. and sp. nov. and the description of a new algal class, the Pelagophyceae classis nov. J. Phycol. 29, 701–715.

Andersen, R.A., Bidigare, R.R., Keller, M.D., Latasa, M., 1996. A comparison of HPLC pigment signatures and electron microscopic observations for oligotrophic waters of the North Atlantic and Pacific Oceans. Deep-Sea Res. Part II 43, 517–537.

Amacher, J., Neuer, S., Anderson, I., Massana, R., 2009. Molecular approach to determine contributions of the protist community to particle flux. Deep-Sea Res. Part I 56, 2206–2215.

Barlow, R.G., Mantoura, R.F.C., Gough, M.A., Fileman, T.W., 1993. Pigment signatures of the phytoplankton composition in the northeastern Atlantic during the 1990 spring bloom. Deep-Sea Res. Part II 40, 459–477.

Barlow, R.G., Mantoura, R.F.C., Cummings, D.G., Fileman, T.W., 1997. Pigment chemotaxonomic distributions of phytoplankton during summer in the western Mediterranean. Deep-Sea Res. Part II 44, 833–850.

Barlow, R.G., Mantoura, R.F.C., Cummings, D.G., 1999. Monsoonal influence on the distribution of phytoplankton pigments in the Arabian sea. Deep-Sea Res. Part II 46, 677–699.

Bidigare, R.R., Chai, F., Landry, M.R., Lukas, R., Hannides, C.C.S., Christensen, S.C., Karl, D.M., Shi, L., Chao., Y., 2009. Subtropical ocean ecosystem structure changes forced by North Pacific climate variations. J. Plankton Res. 31, 1131–1139.

Bidigare, R.R., Ondrusek, M., 1996. Spatial and temporal variability of phytoplankton pigment distributions in the central equatorial Pacific Ocean. Deep-Sea Res. Part II 43, 809–833.

Bidigare, R.R., Van Heukelem, L., Trees, C.C., 2005. Analysis of algal pigments by high-performance liquid chromatography. In: Andersen, R.A. (Ed.), Algal Culturing Techniques. Academic Press, New York, pp. 327–345.

Brzezinski, M.A., Krause, J.W., Church, M.J., Karl, D.M., Li, B., Jone, J.L., Updyke, B., 2011. The annual silica cycle of the North Pacific subtropical gyre. Deep-Sea Res. Part I 58, 988–1001.

Campbell, L., Vaulot, D., 1993. Photosynthetic picoplankton community structure in the subtropical North Pacific Ocean near Hawaii (Station ALOHA). Deep-Sea Res. Part I 40, 2043–2060.

Church, M.J., Ducklow, H.W., Letelier, R.M., Karl, D.M., 2006. Temporal and vertical dynamics in picoplankton photoheterotrophic production in the subtropical North Pacific Ocean. Aquat. Microb. Ecol. 45, 41–53.

Church, M.J., Mahaffey, C., Letelier, R.M., Lukas, R., Zehr, J.P., Karl, D.M., 2009. Physical forcing of nitrogen fixation and diazotroph community structure in the North Pacific Subtropical Gyre. Global Biogeochem. Cycles 23, GB003418, http://dx.doi.org/10.1029/2008.

Claustre, H., Marty, J.C., 1995. Specific phytoplankton biomasses and their relation to primary production in the tropical North Atlantic. Deep-Sea Res. Part I 42, 1475–1493.

Cortés, M.Y., Bollmann, J., Thierstein, H.R., 2001. Coccolithophore ecology at the HOT station ALOHA, Hawaii. Deep-Sea Res. Part II 48, 1957–1981.

Cuvelier, M.L., Allen, A.E., Monier, A., McCrow, J.P., Messie, M., Tringe, S.G., et al., 2010. Targeted metagenomics and ecology of globally important uncultured eukaryotic phytoplankton. Proc. Natl. Acad. Sci. USA 107, 14679–14684.

Daugbjerg, N., Andersen, R.A., 1997. Phylogenetic analyses of the *rbcL* sequences from haptophytes and heterokont algae suggest their chloroplasts are unrelated. Mol. Biol. Evol. 14, 1242–1251.

DeMaster, D.J., 1981. The supply and accumulation of silica in the marine environment. Geochim. Cosmochim. Acta 45, 1715–1732.

DiTullio, G.R., Geesey, M.E., Jones, D.R., Daly, K.L., Campbell, L., Smith, W.O., 2003. Phytoplankton assemblage structure and primary productivity along 170°W in the South Pacific Ocean. Mar. Ecol. Prog. Ser. 255, 55–80.

Dore, J.E., Karl, D.M., 1996. Nitrite distributions and dynamics at Station ALOHA. Deep-Sea Res. Part II 43, 385–402.

Dore, J.E., Brum, J.R., Tupas, L.M., Karl, D.M., 2002. Seasonal and interannual variability in sources of nitrogen supporting export in the oligotrophic subtropical North Pacific Ocean. Limnol. Oceanogr. 47, 1595–1607.

Dore, J.E., Letelier, R.M., Church, M.J., Lukas, R., Karl, D.M., 2008. Summer phytoplankton blooms in the oligotrophic North Pacific Subtropical Gyre: historical perspective and recent observations. Prog. Oceanogr. 76, 2–38.

Fong, A.A., Karl, D.M., Lukas, R., Letelier, R.M., Zehr, J.P., Church, M.J., 2008. Nitrogen fixation in an anticyclonic eddy in the oligotrophic North Pacific Ocean. ISME J. 2, 663–676.

Hebel, D.V., Karl, D.M., 2001. Seasonal, interannual and decadal variations in particulate matter concentrations and composition in the subtropical North Pacific Ocean. Deep-Sea Res. Part II 48, 1669–1695.

Jardillier, L., Zubkov, M.V., Pearman, J., Scanlan, D.J., 2010. Significant CO_2 fixation by small prymnesiophytes in the subtropical and tropical northeast Atlantic Ocean. ISME J. 4, 1180–1192.

Jeffrey, S.W., Wright, S.W., 1994. Photosynthetic pigments in the Haptophyta. In: Green, J.C., Leadbeater, B.S.C. (Eds.), The Haptophyte Algae. Claredon Press, Oxford, U.K., pp. 111–132, p.

John, D.E., Patterson, S.S., Paul, J.H., 2007. Phytoplankton-group specific quantitative polymerase chain reaction assays for RuBisCO mRNA transcripts in seawater. Mar. Biotechnol. 9, 747–759.

Johnson, K.S., Riser, S.C., Karl, D.M., 2010. Nitrate supply from deep to near-surface waters of the North Pacific subtropical gyre. Nature 465, 1062–1065.

Karl, D.M., 1999. A sea of change: biogeochemical variability in the North Pacific Subtropical Gyre. Ecosystems 2, 181–214.

Karl, D.M., Bidigare, R.R., Letelier, R.M., 2001. Long-term changes in plankton community structure and productivity in the North Pacific Subtropical Gyre: the domain shift hypothesis. Deep-Sea Res. Part II 48, 1449–1470.

Karl, D.M., Bidigare, R.R., Letelier, R.M., 2002. Sustained and aperiodic variability in organic matter production and phototrophic microbial community structure in the North Pacific Subtropical Gyre. In: Williams, B., Thomas, D.N., Reynolds, C.S. (Eds.), Phytoplankton Productivity and Carbon Assimilation in Marine and Freshwater Ecosystems. Blackwell, London, pp. 222–264, p.

Karl, D.M., Church, M.J., Dore, J.E., Letelier, R.M., Mahaffey, C., 2012. Predictable and efficient carbon sequestration in the North Pacific Ocean supported by symbiotic nitrogen fixation. Proc. Natl. Acad. Sci. 109, 1842–1849.

Karl, D.M., Lukas, R., 1996. The Hawaii Ocean Time-series (HOT) program: background, rationale and field implementation. Deep-Sea Res. Part II 43, 129–156.

Karl, D.M., Christian, J.R., Dore, J.E., Hebel, D.V., Letelier, R.M., Tupas, L.M., Winn, C.D., 1996. Seasonal and interannual variability in primary production and particle flux at Station ALOHA. Deep-Sea Res. Part II 43, 539–568.

Karl, D.M., 2002. Nutrient dynamics in the deep blue sea. Trends Microbiol. 10, 410–418.

Knauer, G.A., Martin, J.H., Bruland, K.W., 1979. Fluxes of particulate carbon, nitrogen and phosphorus in the upper water column of the northeast Pacific. Deep-Sea Res. 26, 97–108.

Letelier, R.M., Bidigare, R.R., Hebel, D.V., Ondrusek, M., Winn, C.D., Karl, D.M., 1993. Temporal variability of phytoplankton community structure based on pigment analysis. Limnol. Oceanogr. 38, 1420–1437.

Letelier, R.M., Dore, J.E., Winn, C.D., Karl, D.M., 1996. Seasonal and interannual variations in photosynthetic carbon assimilation at Station ALOHA. Deep-Sea Res. Part II 43, 467–490.

Letelier, R.M., Karl, D.M., Abbott, M.R., Flament, P., Freilich, M., Lukas, R., Strub, T., 2000. The role of late winter meso-scale events in the biogeochemical variability of the upper water column of the North Pacific Subtropical Gyre. J. Geophys. Res. 105, 28723–28739.

Letelier, R.M., Karl, D.M., Abbott, M.R., Bidigare, R.R., 2004. Light driven seasonal patterns of chlorophyll and nitrate in the lower euphotic zone of the North Pacific Subtropical Gyre. Limnol. Oceanogr. 49, 508–519.

Li, B., Karl, D.M., Letelier, R.M., Church, M.J., 2011. Size-dependent photosynthetic variability in the North Pacific Subtropical Gyre. Mar. Ecol. Prog. Ser. 440, 27–40.

Li, W.K., 1993. Primary production of prochlorophytes, cyanobacteria, and eucaryotic ultraphytoplankton: measurements from flow cytometric sorting. Limnol. Oceanogr. 39, 169–175.

Ludwig, W., et al., 2004. ARB: a software environment for sequence data. Nucleic Acids Res. 32, 1363–1371.

Mackey, M.D., Mackey, D.J., Higgins, H.W., Wright, S.W., 1996. CHEMTAX a program for estimating class abundances from chemical markers: application to HPLC measurements of phytoplankton. Mar. Ecol. Prog. Ser. 144, 265–283.

Malmstrom, R., Coe, A., Kettler, G.C., Martiny, A.C., Frias-Lopez, J., Zinser, E.R., Chisholm, S.W., 2010. Temporal dynamics of *Prochlorococcus* ecotypes in the Atlantic and Pacific oceans. ISME J. 4, 1252–1264.

Mann, D.G., Simpson, G.E., Sluiman, H.J., Möller, M., 2001. *rbcL* gene tree of diatoms: a second large data-set for phylogenetic reconstruction. Phycologia 40, 1–2.

Marty, J., Chiavérini, J., Pizay, M., Avril, B., 2002. Seasonal and interannual dynamics of nutrients and phytoplankton pigments in the western Mediterranean Sea at the DYFAMED time-series station (1991–1999). Deep-Sea Res. Part II 49, 1965–1985.

Not, F., et al., 2008. Phytoplankton diversity across the Indian Ocean: a focus on the picoplanktonic size fraction. Deep-Sea Res. Part I 55, 1456–1473.

Obayashi, Y., Tanoue, E., Suzuki, K., Handa, N., Nojiri, Y., Wong, C.S., 2001. Spatial and temporal variabilities of phytoplankton community structure in the northern North Pacific as determined by phytoplankton pigments. Deep-Sea Res. Part I 48, 439–469.

Paul, J.H., Pichard, S.L., Kang, J.B., Watson, G.M.F., Tabita, F.R., 1999. Evidence for a clade-specific temporal and spatial separation in ribulose bisphosphate carboxylase gene expression in phytoplankton populations off Cape Hatteras and Bermuda. Limnol. Oceanogr. 44, 12–23.

Paul, J.H., Alfreider, A., Wawrik, B., 2000. Micro- and macrodiversity in *rbcL* sequences in ambient phytoplankton populations from the southeastern Gulf of Mexico. Mar. Ecol. Prog. Ser. 198, 9–18.

Richardson, T.L., Jackson, G.A., 2007. Small phytoplankton and carbon export from the surface ocean. Science 315, 838–840.

Sakamoto, C.M., Karl, D.M., Jannasch, H.W., Bidigare, R.R., Letelier, R.M., Walz, P.M., Ryan, J.P., Polito, P.S., Johnson, K.S., 2004. Influence of Rossby waves on nutrient dynamics and the plankton community structure in the North Pacific subtropical gyre. J. Geophys. Res. (Oceans) 109, C05032, http://dx.doi.org/10.1029/2003JC001976.

Scharek, R., Latasa, M., Karl, D.M., Bidigare, R.R., 1999a. Temporal variations in diatom abundance and downward vertical flux in the oligotrophic North Pacific gyre. Deep-Sea Res. Part I 46, 1051–1075.

Scharek, R., Tupas, L.M., Karl, D.M., 1999b. Diatom fluxes to the deep sea in the oligotrophic North Pacific gyre at Station ALOHA. Mar. Ecol. Prog. Ser. 182, 55–67.

Steinberg, D., Carlson, C., Bates, N., Johnson, R., Michaels, A., Knap, A., 2001. Overview of the US JGOFS Bermuda Atlantic Time-series Study (BATS): a decade-scale look at ocean biology and biogeochemistry. Deep-Sea Res. II 48, 1405–1447.

Suzuki, K., Minami, C., Liu, H., Saino, T., 2002. Temporal and spatial patterns of chemotaxonomic algal pigments in the subarctic Pacific and the Bering Sea during the early summer of 1999. Deep-Sea Res. Part II 49, 5685–5704.

Sverdrup, H.U., Johnson, M.W., Fleming, R.H., 1942. The Oceans. Prentice-Hall, Englewood Cliffs, N. J..

Tabita, F.R., 1999. Microbial ribulose 1,5-bisphosphate carboxylase/oxygenase: a different perspective. Photosynth. Res. 60, 1–28.

Tabita, F.R., Hanson, T.E., Li, H., Satagopan, S., Singh, J., Chan, S., 2007. Function, structure, and evolution of the RubisCO-like proteins and their RubisCO homologs. Microbiol. Mol. Biol. Revolution 71, 576–599.

Treusch, A.H., Demir-Hilton, E., Vergin, K.L., Worden, A.Z., Carlson, C.A., Donatz, M.G., Burton, R.M., Giovannoni, S.J., 2011. Phytoplankton distribution patterns in the northwestern Sargasso Sea revealed by small subunit rRNA genes from plastids. ISME J. 6, 481–492.

Venrick, E.L., 1982. Phytoplankton in an oligotrophic ocean: observations and questions. Ecol. Monogr. 52, 129–154.
Venrick, E.L., 1988. The vertical distribution of chlorophyll and phytoplankton species in the North Pacific central environment. J. Plankton Res. 10, 987–998.
Venrick, E.L., 1990. Phytoplankton in an oligotrophic ocean: species structure and interannal variability. Ecology 71, 1547–1563.
Venrick, E.L., 1992. Phytoplankton species structure in the central North Pacific: is the edge like the center? J. Plankton Res. 14, 665–680.
Venrick, E.L., 1997. Comparison of the phytoplankton species composition and structure in the Climax area (1973–1985) with that of station ALOHA (1994). Limnol. Oceanogr. 42, 1643–1648.
Venrick, E.L., 1999. Phytoplankton species structure in the central North Pacific, 1973–1996: variability and persistence. J. Plankton Res. 21, 1029–1042.
Watson, G.M., Tabita, F.R., 1996. Regulation, unique gene organization, and unusual primary structure of carbon fixation genes from a marine phycoerythrin-containing cyanobacterium. Plant Mol. Biol. 32, 1103–1115.
Wawrik, B., Paul, J.H., Tabita, T.R., 2002. Real-time PCR quantification of *rbcL* (ribulose-1,5-bisphosphate carboxylase/oxygenase) mRNA in diatoms and pelagophytes. Appl. Environ. Microbiol. 68, 3771–3779.
Wawrik, B., et al., 2003. Vertical structure of the phytoplankton community associated with a coastal plume in the Gulf of Mexico. Mar. Ecol. Prog. Ser. 251, 87–101.
White, A.E., Spitz, Y.H., Letelier, R.M., 2007. What factors are driving summer phytoplankton blooms in the North Pacific Subtropical Gyre? J. Geophys. Res. 112, C12006.
Worden, A.Z., Janouskovec, J., McRose, D., Engman, A., Welsh, R.M., Malfatti, S., Tringe, S.G., Keeling, P.J., 2012. Global distribution of a wild alga revealed by targeted metagenomics. Curr. Biol. 22, R675–R677.
Worden, A.Z., Nolan, J.K., Palenik, B., 2004. Assessing the dynamics and ecology of marine phytoplankton: the importance of the eukaryotic component. Limnol. Oceanogr. 49, 168–179.
Zhang, H., Lin, S., 2005. Development of a *cob*-18S rRNA gene real-time PCR assay for quantifying *Pfiesteria shumwayae* in the natural environment. Appl. Environ. Microbiol. 71, 7053–7063.